Swansea University
Prifysgol Abertawe

Cronfa
Setting Research Free

Cronfa - Swansea University Open Access Repository

This is an author produced version of a paper published in:
Surface and Interface Analysis

Cronfa URL for this paper:
http://cronfa.swan.ac.uk/Record/cronfa50778

Paper:
Holliman, P., Hill, D., Appelman, M., Chatterjee, P., McGettrick, J., Jones, E. & Worsley, D. (in press). Desorption of carboxylates and phosphonates from galvanized steel: towards greener lubricants. *Surface and Interface Analysis*
http://dx.doi.org/10.1002/sia.6681

This item is brought to you by Swansea University. Any person downloading material is agreeing to abide by the terms of the repository licence. Copies of full text items may be used or reproduced in any format or medium, without prior permission for personal research or study, educational or non-commercial purposes only. The copyright for any work remains with the original author unless otherwise specified. The full-text must not be sold in any format or medium without the formal permission of the copyright holder.

Permission for multiple reproductions should be obtained from the original author.

Authors are personally responsible for adhering to copyright and publisher restrictions when uploading content to the repository.

http://www.swansea.ac.uk/library/researchsupport/ris-support/

Received: 15 January 2019 | Revised: 1 June 2019 | Accepted: 5 June 2019

DOI: 10.1002/sia.6681

RESEARCH ARTICLE

WILEY SURFACE and INTERFACE ANALYSIS

Desorption of carboxylates and phosphonates from galvanized steel: Towards greener lubricants

Donald Hill[1] | Peter J. Holliman[1] | Eurig W. Jones[1] | James McGettrick[1] | David A. Worsley[1] | Marco Appleman[2] | Pranesh Chatterjee[2]

[1] College of Engineering, Bay Campus, Swansea University, Swansea, UK

[2] Tata Steel Research and Development, Ijmuiden, The Netherlands

Correspondence
Peter J. Holliman, College of Engineering, Bay Campus, Swansea University, Swansea SA1 8EN, UK.
Email: p.j.holliman@swansea.ac.uk

Funding information
Engineering and Physical Sciences Research Council, Grant/Award Numbers: EP/M015254/1, EP/M028267/1 and EngD; Welsh Government, Grant/Award Number: Ser Cymru; Ser Solar project; European Regional Development Fund, Grant/Award Number: 80708; EPSRC, Grant/Award Number: EP/M028267/1; SPACE-modules; Welsh Government for Sêr Cymru; EPSRC EngD and Tata Steel

This paper studies the removal of chemisorbed carboxylates and phosphonates from TiO_2-coated galvanized steel using $NaOH_{(aq)}$. XPS and FTIR data show that $NaOH_{(aq)}$ is effective at desorbing these species and so is an alternative to gas phase processes (eg, plasma cleaning). Tribological investigations show that $NaOH_{(aq)}$-treated surfaces show reduced friction and wear, relative to the "as-received" galvanized steel. This is ascribed to carbonate (present as an impurity in NaOH) that adsorbs to the surface of the substrate during $NaOH_{(aq)}$ immersion. Carbonate removal through sonication in water generates surfaces that show friction similar to "as-received" galvanized steel. This work is useful in areas (eg, automotive manufacturing), where the effective removal of lubricants following tribological contact is key to subsequent paint adhesion.

KEYWORDS

carbonate, inherent lubricity, plasma cleaning, surfaceswear

1 | INTRODUCTION

Functionalization of surfaces with chemisorbed molecules is an attractive route to tailor interfacial properties such as lubricity[1-3] and wetting.[2-5] Self-assembled monolayers (SAMs) have been widely used in recent years to this end due to their durability and relative ease of preparation.[1] Reports shows that SAMs form on a variety of surfaces; eg, Al_2O_3[2] or copper oxide,[3,5] SiO_2,[6,7] and metals like Au[4,8] and Ag.[9,10] Molecules that form SAMs possess a linker group that can interact with surface sites (eg, CO_2H or SH) and an alkyl or perfluoroalkyl chain that points away from the surface.[1,7] Condensation reactions between the linker groups and surface sites[7] create covalent bonds, and the resultant SAMs lower the surface energy and provide a physical barrier against tribological contact to improve abrasion performance and chemical resistance.[1,11]

SAMs are reported to lower the coefficient of friction (μ) of substrates by a molecular spring mechanism, where the orientation of the spacer chains reduces interfacial shear forces.[1,12] Hence, SAMs have been cited as possible lubricants for small length scales tribological contacts; eg, micro/nano-electromechanical systems (MEMS/NEMS)[1,5,13] and in sheet metal forming processes[3] which are used in the automotive, building, and aviation industries to create shaped components.

Oils and oil-based lubricants are widely used to reduce friction in these processes.[14,15] Thicknesses of these lubricant films are dictated by the surface roughness of the materials[3] that are undergoing plastic deformation, because it is necessary that the lubricant covers all of the surface features in order to prevent wear. In practice, this leads to an over compensation of the amount of lubricant that is applied, which increases cost and waste because excess lubricant must then be removed to prevent impacting on subsequent sheet metal forming operations (eg, painting, welding[16]).

Previous work has shown that alkyl carboxylic[2] or phosphonic acids[3] can be used to imbue inherent lubricity to Al or copper oxide

This is an open access article under the terms of the Creative Commons Attribution License, which permits use, distribution and reproduction in any medium, provided the original work is properly cited.
© 2019 The Authors Surface and Interface Analysis Published by John Wiley & Sons Ltd

substrates. In addition, despite the large number of studies reporting SAM formation, there are relatively few reports of how SAMs can be removed from surfaces. The few reports there are describe thiol removal from Au using gas-phase processes (eg, plasma cleaning[8] and ozonolysis[17,18]) or electrochemical methods.[19-21] By comparison, there are few reports describing carboxylate or phosphonate SAM removal from metal substrates although the removal of carboxylates from TiO_2 surfaces has been achieved through de-esterification, using bases like NaOH and Bu_4NOH.[22]

This study investigates the desorption of chemisorbed lauric ($R_{12}C$) and dodecylphosphonic acid ($R_{12}P$) from TiO_2-coated automotive-grade galvanized steels using $NaOH_{(aq)}$. Detailed surface characterization (X-ray photoelectron and infrared [IR] spectroscopy) allied to water contact angle (WCA) measurements to study surface wetting have been combined with scanning electron microscopy to study how $NaOH_{(aq)}$ treatment affects the galvanized steel surface. These data have been correlated with the tribological properties of the functionalized and NaOH-treated surfaces using linear friction testing (LFT) and confocal microscopy. In order to study the effectiveness of $NaOH_{(aq)}$ as a method of removing these chemisorbed species, we have evaluated this method against O_2 plasma cleaning. Exposure of surface-adsorbed species to O_2 plasma has been shown to be an effective method of removing compounds from surfaces.[8] Consequently, it was used as comparison to study the efficacy of the $NaOH_{(aq)}$ treatment.

2 | EXPERIMENTAL METHODS

2.1 | Substrate and surface treatments

Hot-dip galvanized (HDG) steel substrate (DX56, Tata Steel) was sheared into 10 × 20 mm^2 coupons for characterization and 50 × 300 mm^2 strips for LFT. The steel composition (%wt) was Al 0.036, C 0.0022, Mo 0.001, Ni 0.001, N 0.0035, P 0.009, Si 0.003, S 0.010, Sn 0.004, Ti 0.050, V 0.002, Cr 0.012, Cu 0.026, Mn 0.088, B 0.002 (balance was Fe). During galvanizing, the steel immersed in a bath of molten Zn containing 0.3% wt Al. Consequently, the surface galvanic layer is 99.7% Zn. All chemicals (Sigma-Aldrich) were used without purification. The HDG steel substrate was coated with TiO_2 using an isopropanolic solution of Ti $(O_iPr)_4$ (100 mM) for 30 seconds before drying in air for 1 minute as described previously.[23,24] Samples were then immersed in 100 mM isopropanolic solutions of dodecanoic acid ($R_{12}C$) or dodecane phosphonic acid ($R_{12}P$) for 30 seconds and allowed to air dry. Physisorbed species were removed from the surfaces through rinsing the coated substrates with acetone for several minutes. Bands ascribed to physisorbed species (eg, C═O and O) were not observed after rinsing using IR spectroscopy. This indicated that the residual material was chemisorbed onto the surface. Desorption of chemisorbed $R_{12}C$ and $R_{12}P$ was achieved through immersing the acetone-washed surfaces in 100 mM NaOH (aq). Selected samples were then sonicated in deionized H_2O for 1 minute followed by drying in air. Plasma cleaning was carried out using a radio frequency induced O_2 plasma in an Electronic Diener plasma cleaner. Before cleaning, the chamber was placed under vacuum (< 1 mbar) before the O_2 was injected (pressure < 10 mbar) and the samples exposed for 10 minutes on each side.

2.2 | Characterization

Attenuated total reflectance Fourier transform infrared (ATR-FTIR) spectroscopy was carried out on a Perkin Elmer 100 Series spectrometer (four scans, 4 cm^{-1} resolution, 650-4000 cm^{-1}). Sessile drop WCA measurements (n = 5, 5-μL droplets) were conducted with a USB 2.0 camera and goniometer using FTA 32 software (FTA 32 Europe). X-ray photoelectron spectroscopy (XPS) was studied using an Axis Supra XPS (Kratos Analytical) with a monochromated Al Kα source and large area slot mode detector (*ca*. 300 μm × 800 μm analysis area). Charge neutralization was used to limit differential charging, and the data calibrated with respect to the C 1s peak (284.8 eV). Survey spectra (step size 1 eV, dwell time 0.1 second, pass energy 160 eV) were collected at three surface locations before high-resolution spectra (step size 0.1 eV, dwell time 250 ms, pass energy 20 eV). Data were fitted using CASA software and Shirley backgrounds. Field emission gun scanning electron microscopy (FEG-SEM) was studied using a Hitachi S4800 at 1.0 kV. Confocal microcopy was performed at 20× magnification (2.1 × 2.1 mm field of view) on a Nanofocus μSurf Mobile microscope. Topographic images were plotted using Mountains software (version 7.3). XRD was performed on a Bruker D8 Discover Diffractometer using Cu K_α radiation (λ = 0.15406 nm) at 0.0196° step size. Zinc concentrations were measured by atomic absorbance spectroscopy (AAS) on a Varian SpectrAA 220FS (λ = 213.9 nm, current = 5 mA slit width = 0.1 nm slit) using an acetylene flame. The instrument was calibrated using seven standards from 0 to 2000 Zn^{2+} μg L^{-1} diluted from a standard Zn solution containing 1%wt HCl (Sigma-Aldrich). LFT was measured (n = 3) over a length of 60 mm by pulling a strip of steel through flat and cylindrical tools at an average velocity of 0.345 mm s^{-1}. The tools were clamped together using a force of 5 kN. The coefficient of friction (μ) was calculated using Equation (1) where F_t is the pulling force whilst F_N is the clamping force. The average μ values were recorded at the 40 to 50-mm region of the sample because static friction often dominated the first 20 mm of sliding. Full details of the LFT testing are given ESI 1.0.

$$\mu = F_t/(2 \times F_N) \quad (1)$$

3 | RESULTS AND DISCUSSION

3.1 | Surface characterization

The surface composition and morphology of the TiO_2 coated HDG-steel substrate have been in detail previously.[24] After deposition of $R_{12}C$, the ATR-IR data show C—H stretching and bending bands of

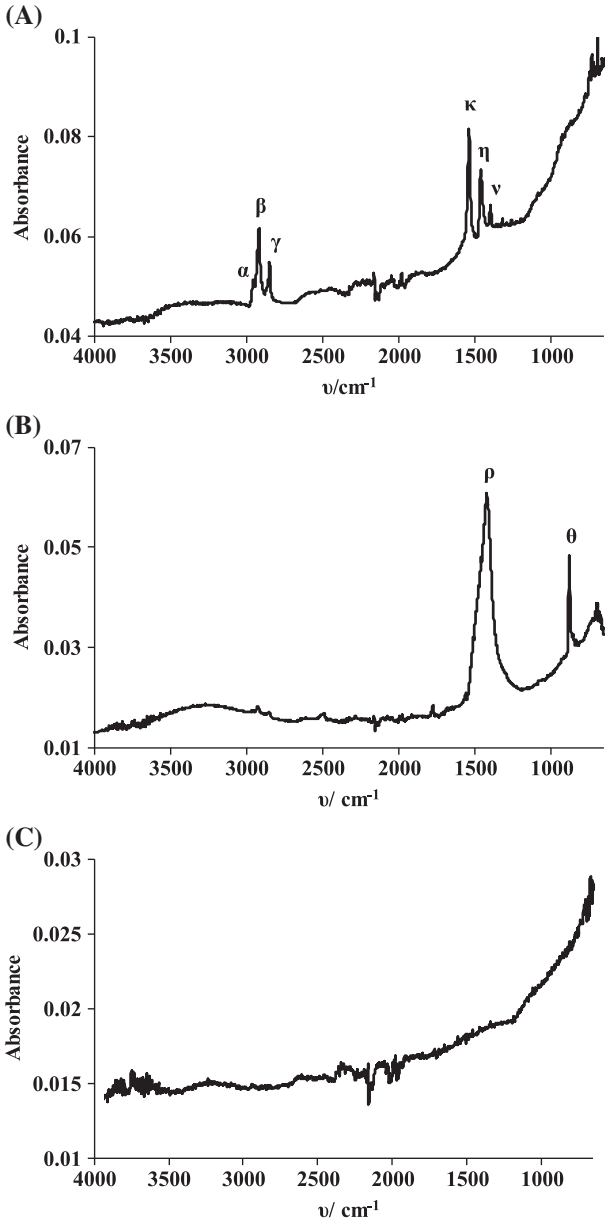

FIGURE 1 ATR-IR spectra of the $R_{12}C$ functionalized surface A, after $R_{12}C$ deposition, B, after immersion in $NaOH_{(aq)}$, and C, after immersion in $NaOH_{(aq)}$ and sonication in H_2O. α = CH_3 asymmetric stretch, β = υ CH_2 asymmetric stretch, γ = υ CH_2 symmetric stretch, κ = carboxylate asymmetric stretch, η = CH_2 bend, ν = carboxylate symmetric stretch, ρ = υ CO_3^{2-} asymmetric stretch, and θ = υ CO_3^{2-} out-of-plane bend

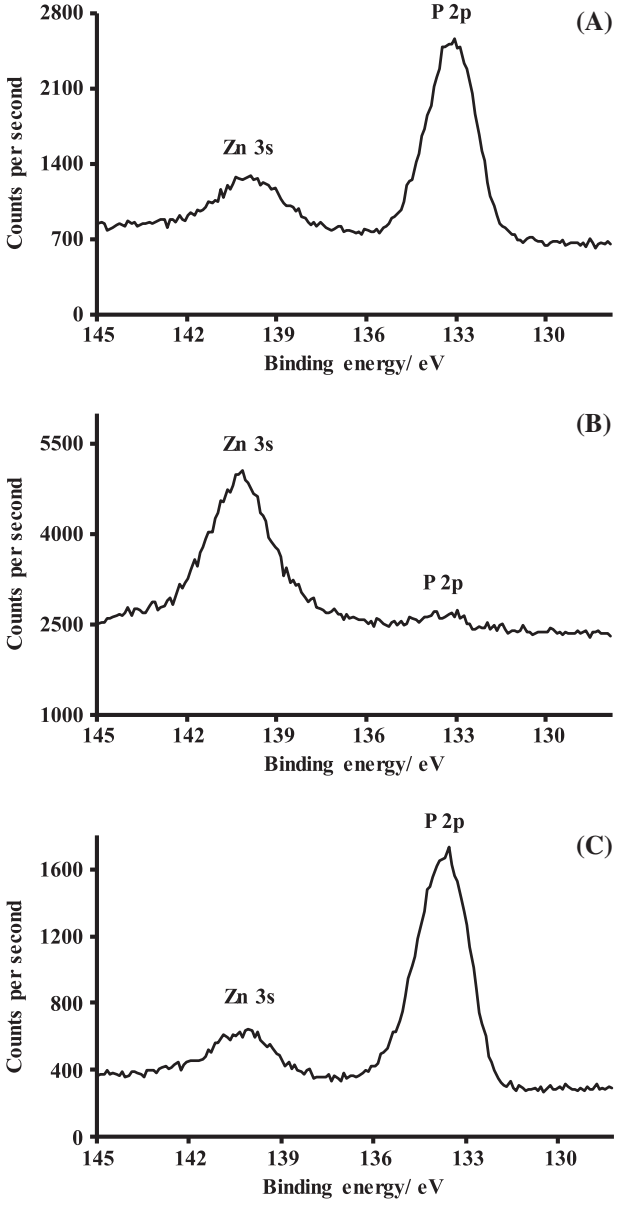

FIGURE 2 High-resolution XPS data of the Zn 3s and P 2p regions on the $R_{12}P$ functionalized surface A, after $R_{12}P$ deposition, B, after immersion in $NaOH_{(aq)}$, and C, after O_2 plasma cleaning

the alkyl chain,[25] along with asymmetric and symmetric carboxylate stretching bands for the linker group at 1540 and 1398 cm^{-1}, respectively[26-28] (Figure 1A). The wavenumber gap between these carboxylate stretching bands suggests bridging mode coordination.[27] However, after immersion in $NaOH_{(aq)}$, only very weak CH_2 symmetric and asymmetric stretching bands are observed after the $R_{12}C$ functionalized surface was immersed in the $NaOH_{(aq)}$ (Figure 1B). This suggests that almost all the $R_{12}C$ was desorbed but there may have been a trace amount of $R_{12}C$ which was not desorbed during the treatment. It was not possible to unequivocally confirm this because carboxylate stretching bands are coincident with the new and more intense carbonate asymmetric stretching band observed in the IR spectrum[29] (Figure 1B). The trace CH_2 bands were not observed in the IR spectrum of the NaOH-treated surface after sonication in H_2O, which could suggest that they were ascribed to a species that could be removed due to sonication. For the newly observed carbonate bands, these are ascribed to the *ca*. 2% impurity of Na_2CO_3 that typically forms in NaOH during its manufacturing. Hence, these data show that the substrate is altered so that carbonate species end up on the substrate surface during the base-catalyzed desorption of $R_{12}C$ in $NaOH_{(aq)}$. The bands ascribed to carbonate stretching and bending modes (1422 and 879 cm^{-1}, respectively) are at similar positions to as in the IR spectrum of pure sodium bicarbonate.[26] Consequently, it is not possible to ascertain from the FTIR data

what carbonate species is on the surface; ie, whether it is a new carbonate phase. However, what is known is that the carbonate ion (CO_3^{2-}) is a planar molecule with no alkyl chains like $R_{12}C$ or $R_{12}P$. Hence, if it does adsorb, it could either be perpendicular to the surface or in planar configuration. The SEM data (Figure 4) do show rod-like features which do suggest a separate carbonate phase. Interestingly, it is known that carbonates can imbue lubricity when added as lubricant additives[30,31] which is in line with the later coefficient of friction testing for these surfaces.

In addition, in the 100 mM $NaOH_{(aq)}$ solution, the pH is 13 which greatly exceeds the pK_a values for lauric acid (pK_a = 5.3) or sodium bicarbonate (pK_{a1} = 6.4, pK_{a2} = 10.3) meaning that all ions are fully dissociated. In addition, the 100 mM concentration of hydroxyl ions from NaOH will greatly exceed the number of adsorbed molecules which helps drive the desorption process. At the same time, the *ca*. 2% carbonate impurity in NaOH results in *ca*. 2 mM of CO_3^{2-}. A partitioning process between $CO_3^{2-}{}_{(aq)}$ and $CO_3^{2-}{}_{(sorbed)}$ will take place. Our previous work on dyeing metal oxides[22] shows that 2 mM is more than sufficient to drive partitioning towards adsorbed species. Thus, whilst chemical desorption of carbonate was not possible in $NaOH_{(aq)}$, sonication of the $NaOH_{(aq)}$-treated samples in H_2O resulted in no carbonate stretching or bending bands in the ATR-IR spectra (Figure 1C). Instead, the data are very similar to that of the "as-received" HDG substrate (ESI Figure 2). This shows that adsorbed carbonate could be removed from the surface through sonication. Whilst it is possible that sonication could selectively remove adsorbed carbonate, it is more likely that weakly held particles of surface zinc oxide are physically removed and the carbonate inevitably is removed along with this. This creates a pristine zinc metal surface which does not dissolve because the pH of the water is neutral and instead rapidly re-oxidizes to ZnO.

The IR spectrum for the $R_{12}P$-treated sample (ESI Figure 3A) shows C—H stretching and bending modes from the alkyl chain of $R_{12}P$, and asymmetric and symmetric P—O stretching bands (1156 and 1083 cm^{-1}, respectively) from the linker group.[3,32] However, the absence of a O stretching band at ca. 1220 cm^{-1} suggests the phosphonate chemisorbs by tridentate coordination as observed in previous studies.[23,24] After immersion of the substrate in $NaOH_{(aq)}$, no $R_{12}P$ bands are observed, and only carbonate stretching and bending modes are present (ESI Figure 3b) as for the analogous $R_{12}C$ sample. This indicates that the phosphonate had desorbed from the surface and has been replaced by adsorbed carbonate.

Due to the ubiquitous presence of adventitious C on surfaces, it was not possible to unambiguously determine whether $NaOH_{(aq)}$ had desorbed $R_{12}C$ from the surface using XPS data. The positions of the O—C═O peaks in the XP spectra of an untreated $R_{12}C$ and an $R_{12}C$ sample after immersion in the $NaOH_{(aq)}$ were both observed at 288.9 eV. Consequently, it is not possible to differentiate whether the carbonaceous material remaining on the surface was $R_{12}C$, carbonate, or some other form of adventitious carbon from the XPS data. However, the atomic % values for C, Zn, and Ti observed for $R_{12}C$ samples after $NaOH_{(aq)}$ treatment were similar to the unfunctionalized substrate (Table 1) which suggests that $NaOH_{(aq)}$ does desorb $R_{12}C$ from the surface, in line with the IR data. The Zn:C ratio of the $NaOH_{(aq)}$-treated sample also changes to 0.9:1.0 from 0.7:1.0 for the $R_{12}C$-treated sample which is a closer ratio to the untreated sample (1.2:1.0) but not identical which is ascribed to carbon from the surface carbonate which the IR data show is present after $NaOH_{(aq)}$ treatment (Table 1). The desorption of $R_{12}P$ was also further studied by XPS. After $R_{12}P$ deposition, the XPS data (Figure 2A) show 2s and 2p phosphorus peaks at 191.3 and 133.7 eV, respectively. Notably, these values are in agreement with related studies that report phosphonate

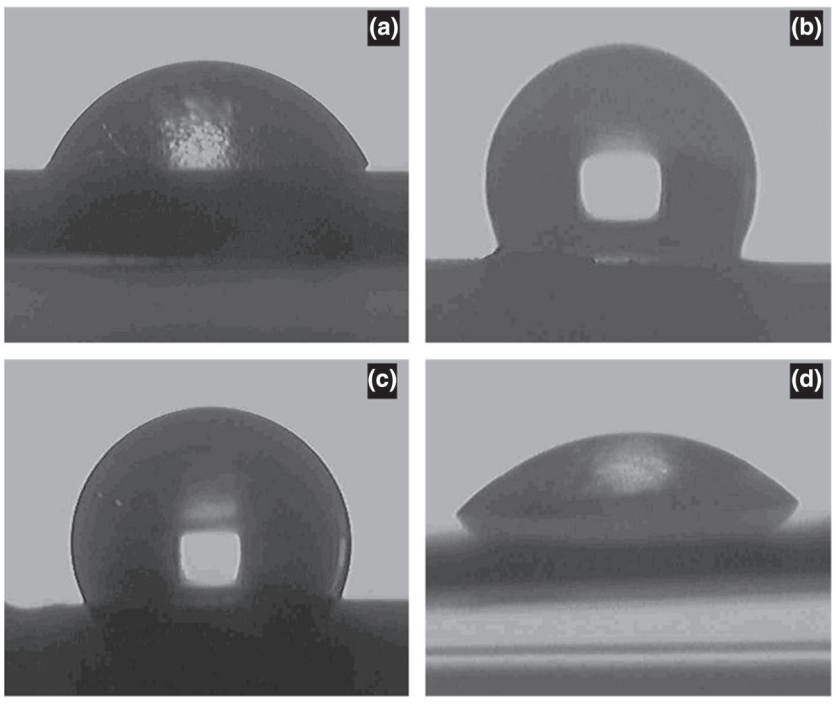

FIGURE 3 Water contact angle images for HDG substrate A, after initial cleaning, B, after $R_{12painitng}C$ deposition, C, after $R_{12}P$ deposition, and D, after $NaOH_{(aq)}$ treatment

TABLE 1 Atomic percentages (calculated using sensitivity factors) and Zn:C ratios calculated the combined areas of the Zn 2p1/2 and Zn 2p 3/2 peaks versus the C 1s peak from XPS on selected surfaces (data are average of three analyses per surface ± standard deviation). Trace contaminants (Si, N, Na, Ca) on TiO_2-coated HDG and on the $R_{12}C$ surfaces were ascribed to contamination from laboratory gloves[33]

	Atomic %		
Element	TiO_2-Coated HDG	$R_{12}C$ Coating	$R_{12}C$ Coating + NaOH
C	58.4 ± 0.8	74.5 ± 1.3	61.2 ± 9.0
Zn	1.9 ± 0.2	1.7 ± 0.0	5.4 ± 1.8
Ti	6.3 ± 0.1	1.2 ± 1.0	3.7 ± 1.2
O	28.5 ± 0.3	20.1 ± 1.2	27.7 ± 7.6
Zn:C	1.2:1.0	0.7:1.0	0.9:1.0

binding on alloy and metal oxide surfaces.[3,34] After $NaOH_{(aq)}$ treatment, very weak phosphorus peaks are observed in the high-resolution XP spectrum. However, the atomic percentage of P was observed to be 0.0 ± 0.0% using CASA XPS software which indicates that the amount of P remaining after the $NaOH_{(aq)}$ treatment is below the limit of detection of the software. This suggests that, at least the majority of, the chemisorbed phosphonates are removed from the surface during this treatment, in line with the IR data. Analysis of the C 1s XPS spectra was also performed. However, the line shapes of the C 1s peak envelopes of surfaces before and after the $NaOH_{(aq)}$ treatment were very similar. Consequently, this made it very difficult to elucidate the nature of the carbonaceous material present on the surfaces.

Water contact angle (WCA) data of the HDG substrate (Figure 3 and Table 2) were 63.2 ± 6.2°, which increases to values between 105° and 115° following chemisorption of $R_{12}C$ or $R_{12}P$ as reported in previous studies.[3,25] After $NaOH_{(aq)}$ treatment, the surfaces became substantially more hydrophilic (WCA < 50°) which is ascribed to the presence of surface adsorbed carbonate. Carbonate is a charge ion with polarized carbon-oxygen bonds which will hydrogen bond to water reducing the surface energy and increasing hydrophilicity. Finally, after sonication in H_2O, the WCA data for either $R_{12}C$ or $R_{12}P$ samples were very similar to the untreated HDG substrate suggesting that both chemisorbed $R_{12}C$ and $R_{12}P$, and carbonate had been removed the surfaces. Surface roughness data have also been measured using confocal microscopy for these treatments (Table 2). The data do not show any substantial changes between the treatments, and so this is not thought to be a major influence on the hydrophobicity or surface lubricity of these samples.

TABLE 2 Water contact angles and arithmetic mean surface roughness (S_a) values of selected treatments. S_a values are calculated from 2.1 × 2.1 mm^2 confocal images

Sample	Water Contact Angle, °	Surface Roughness (S_a), μm
HDG substrate	63.2 ± 6.2	1.34
$R_{12}C$	107.4 ± 5.824	1.46
$R_{12}P$	103.0 ± 4.0[23]	1.48
NaOH-treated HDG substrate	< 50	1.23

SEM of the HDG steel substrate before and after immersion in $NaOH_{(aq)}$ was studied to investigate to effects of the $NaOH_{(aq)}$ solution on the zinc galvanic layer of the substrate. The data show that the surface of the $NaOH_{(aq)}$-treated substrate (Figure 4B) is substantially rougher than the as-received HDG steel (Figure 4A). This suggests that, in addition to desorbing $R_{12}C$ and $R_{12}P$, when the surface is treated with $NaOH_{(aq)}$, the amphoteric surface ZnO dissolves. This exposes the underlying zinc metal which is also dissolved by the $NaOH_{(aq)}$ solution. AAS was used to further study this. The zinc concentration in the initial $NaOH_{(aq)}$ solution was 275 μg Zn L^{-1} which is ascribed to trace impurities during its manufacture. This zinc concentration increases to 1404 μg Zn L^{-1} for $R_{12}C$ and 1704 μg Zn L^{-1} for $R_{12}P$ (ESI Figure 4). Taking into account the increase in zinc concentration and the 100 mL of $NaOH_{(aq)}$ used, this suggests that 112.9 μg of Zn was removed from the $R_{12}C$ sample and 142.9 μg of Zn from the $R_{12}P$ sample. This confirms that $NaOH_{(aq)}$ removes Zn from the HDG steel through etching, and this affects the surface morphology of the material, in line with previously reported data.[35] Assuming a 99.7% zinc galvanic coating of 7 to 10 μm, the total zinc present on 1 × 2 cm samples will be ca. 10 to 14 mg. As such, these data suggest that ca. 10% of the galvanic zinc layer is removed during this etching process. Rod-like features (labelled α but present all over the surface in Figure 4B) were also observed in some areas of the $NaOH_{(aq)}$-treated galvanized steel. XRD data of these samples showed no new diffraction peaks relative to the untreated HDG substrate (ESI Figure 5), suggesting that this material was either poorly crystalline or amorphous. Alternatively, it could be re-deposited Zn and/or ZnO which would not show up as extra peaks because these phases were already present in the HDG-steel substrate. Figure 4C then shows SEM data for $R_{12}C$-coated HDG which has been acetone washed and then NaOH treated. The data do not show the same rod-like features which are observed on the NaOH-treated HDG. Instead, the NaOH-treated $R_{12}C$ surface appears more like TiO_2-coated HDG (Figure 4A) albeit slightly more textured which would be expected after a strong alkali treatment of a zinc-rich surface.

By comparison, the WCAs of the $R_{12}C$ and $R_{12}P$ functionalized surfaces after O_2 plasma cleaning were 58.4 ± 4.0° and 27.2 ± 16.9°. These low WCA values show that the surface is changed by the O_2 plasma and suggest that more organic material is removed presumably by oxidation to produce surface largely composed of metal oxide.[8,36]

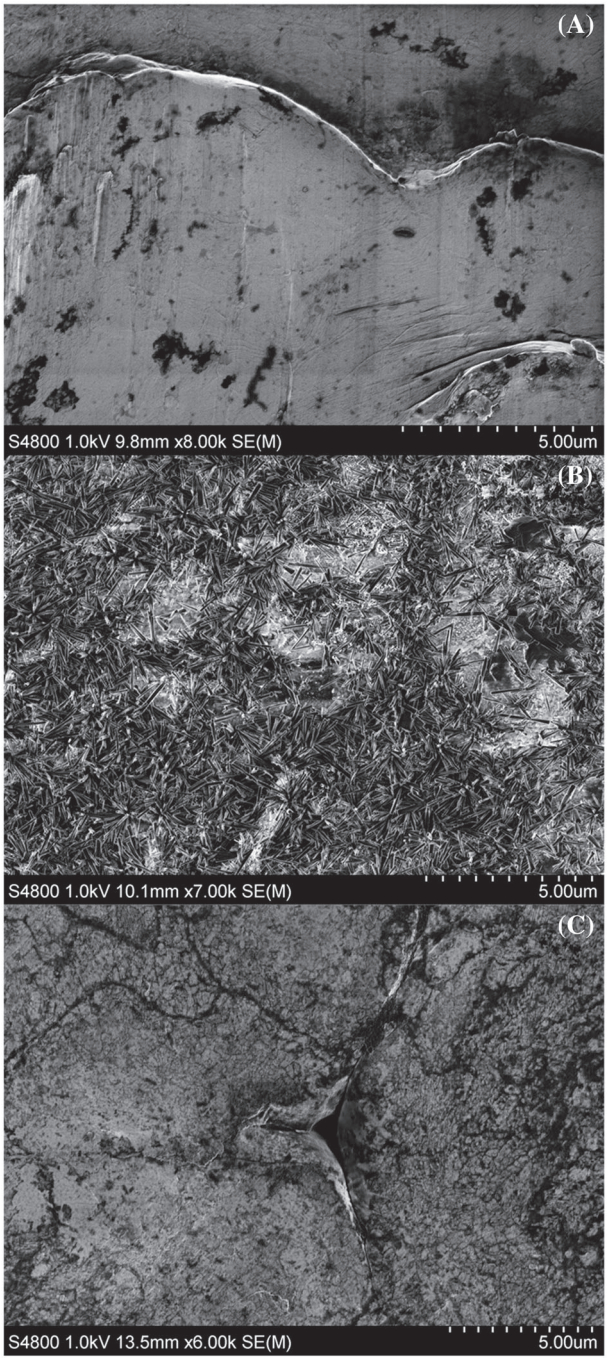

FIGURE 4 FEG-SEM images of HDG-steel substrate A, "as received," B, HDG-steel after immersion in $NaOH_{(aq)}$, and (C) $R_{12}C$-coated HDG after immersion in $NaOH_{(aq)}$

In line with this, the IR spectra of the plasma-cleaned surfaces show very weak C—H stretching bands, indicating that the majority of the chemisorbed organic material had been removed by the plasma (ESI Figure 6). However, XPS data of the NaOH-treated $R_{12}P$ sample still show the presence of P 2s and P 2p photoelectron peaks, suggesting that the phosphonate linker group remains on the surface (Figure 2C). The ratio of the peak areas of the P 2p to the adjacent Zn 3s peak (P:Zn) of this sample was observed to be 4.8:1. An untreated $R_{12}P$ sample was observed to display a P:Zn of approximately 3.1:1, whereas an $R_{12}P$ sample immersed in the $NaOH_{(aq)}$ displayed a P:Zn of 0.0:1. Because the P:Zn of the plasma-cleaned sample is more similar to the untreated $R_{12}P$ sample, this could suggest that the O_2 plasma is ineffective at removing the linker group from the surface. This can be explained because O_2 plasmas oxidize carbonaceous matter so that it is lost as CO_2.[33] However, the P in phosphate is already fully oxidized, and, because it is chemisorbed to the surface, it is not volatile. This explanation is in line with related studies, which have reported the generation of sulfonate species when O_2 plasma was used to remove thiols from Au.[8] In support of this hypothesis, the atomic percentage of C observed on the plasma-cleaned $R_{12}P$ sample was observed to be 57.4 ± 1.7%. The atomic percentage of C observed on the acetone-washed, but not plasma-treated $R_{12}P$ sample, was observed to be 74.2 ± 2.7%, suggesting that the alkyl chain of the phosphonate is removed by the O_2 plasma. By comparison, the XPS data of the $R_{12}P$ functionalized specimen after immersion in the $NaOH_{(aq)}$ show very little P, indicating that the NaOH treatment is a more effective method for removing chemisorbed $R_{12}P$ from the substrate.

3.2 | Tribological testing

The tribological properties of the surfaces were studied using LFT. As discussed in our previous studies, LFT is an aggressive tribological test that is designed to simulate the sliding conditions galvanized steels experience during sheet metal forming operations.[22,23] The data show the average coefficient of friction (μ) of the TiO_2-coated HDG steel substrate is 0.26 ± 0.06. Treatment of the substrate with either $R_{12}C$ or $R_{12}P$ reduced μ to 0.11 ± 0.01 (Figure 5A,B). This large reduction is ascribed to alkyl chains of $R_{12}C$ or $R_{12}P$ acting like molecular springs or brushes during tribological contact.[1,11]

Interestingly, the μ values of the $R_{12}C$ and $R_{12}P$ functionalized surfaces did not increase significantly after immersion in $NaOH_{(aq)}$. This suggests that the carbonate that adsorbs to the surface during caustic treatment provides a lubrication effect and acts as an effective barrier against surface asperity contact. To study this further, LFT measurements were also performed on $NaOH_{(aq)}$-treated surfaces that had been sonicated in H_2O (which our ATR-IR data show removes the adsorbed carbonate). The LFT data show that the average μ value of the surfaces increases substantially after sonication to between 0.17 and 0.25 (Figure 5A,B). These data do suggest that carbonate is responsible for the lower μ values and so does imbue surface lubricity in its own right. In line with this, confocal microscopy shows substantially deeper scratches on the sonicated surfaces relative to samples that were solely subjected to $NaOH_{(aq)}$ (Figure 5C-E). This severe galling behaviour[14] observed after carbonate removal further supports the hypothesis that carbonate does provide a barrier layer that protects the surfaces in motion from wear.

Confocal microscopy has been measured on samples before and after LFT testing. The confocal micrographs and line scans are shown in ESI Figures 7 to 14, whilst Table 3 shows surface roughness data. Before LFT, the arithmetic mean surface roughness (S_a) varies from

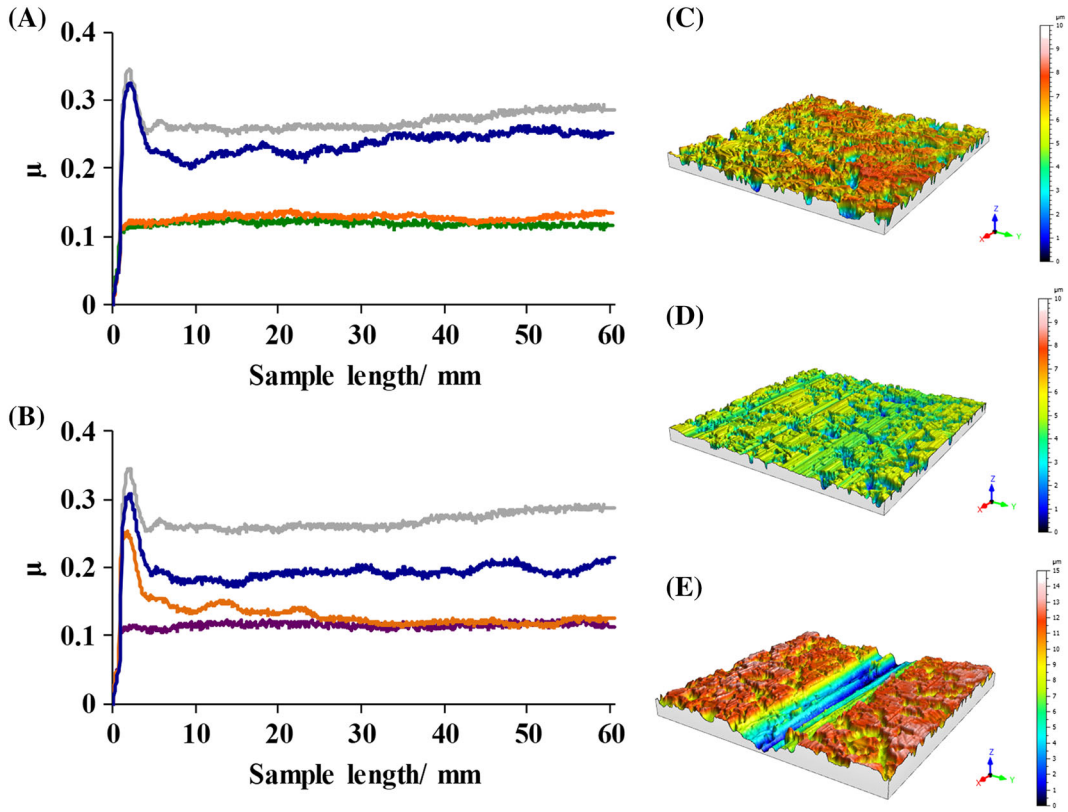

FIGURE 5 Coefficients of friction (μ) versus sliding distance for A, $R_{12}C$ and B, $R_{12}P$-treated surfaces. Data are: TiO_2-coated HDG (grey), $R_{12}C$ (green), $R_{12}P$ (purple), $NaOH_{(aq)}$-treated surfaces (orange), and samples sonicated in H_2O (blue). Confocal micrographs (2.0 × 2.0 mm) of the $R_{12}C$ substrates after LFT measurements C, after $R_{12}C$ deposition, D, after $NaOH_{(aq)}$ treatment, and (E) after sonication in H_2O. Data are from the surface in contact with the flat tool. Scale bars are 10 μm for C, and D, and 15 μm for E,

TABLE 3 Arithmetic mean surface roughness (S_a) values of selected treatments. S_a values are calculated from 2.1 × 2.1 mm^2 confocal images of surfaces in contact with the flat tool

Treatment	Sonicated in H_2O?	Surface Roughness (S_a)	
		Before LFT (μm)	After LFT (μm)
TiO_2-coated HDG	No	1.21	1.54
$R_{12}C$	No	1.46	1.47
$R_{12}P$	No	1.48	1.05
$R_{12}C$ + $NaOH_{(aq)}$	No	1.20	0.96
$R_{12}P$ + $NaOH_{(aq)}$	No	1.44	1.14
$R_{12}C$ + $NaOH_{(aq)}$	Yes	1.35	2.58
$R_{12}P$ + $NaOH_{(aq)}$	Yes	1.23	2.72

1.20 to 1.46 μm across all the samples so there is little difference between the samples. However, after one LFT pass, the $R_{12}P$ sample and the $R_{12}C$ and $R_{12}P$ samples show a small drop in Sa values to 0.96 to 1.14 μm. This is ascribed to a polishing effect where the LFT tool removes extreme surface asperities to effectively smooth the surface (although this is a small effect). By comparison, the $NaOH_{(aq)}$-treated $R_{12}C$ and $R_{12}P$ samples which have been sonicated show an increase in Sa to 2.58 to 2.72 μm. This is ascribed to the removal of surface carbonate particles by sonication, which increases the coefficient of friction and results in more surface damage during the LFT pass.

3.3 | The potential for green lubricants

This work has used a TiO_2 coating onto the galvanized layer as a mimic for Cr-free anticorrosion coatings. Whilst the carboxylate or phosphonate linkers can chemisorb to this metal oxide surface, the native oxide of the galvanic zinc layer can also act in this role. In theory, this makes the TiO_2 layer optional in terms of lubricity which would save a processing step if this layer was not included. However, it is very important for corrosion protection which is why we have included it in this work.

For a lubricant to be considered environmentally sustainable, the active component must be recoverable and reusable. Our data show that the $R_{12}C$ carboxylate and $R_{12}P$ phosphonate can be desorbed from the surfaces in aqueous alkaline solution. Neutralizing these desorbed solutions will enable the compounds to be re-used. The data also show some dissolution of the galvanic zinc layer in the $NaOH_{(aq)}$ during $R_{12}C$ and $R_{12}P$ desorption. Importantly, less than 10% of the galvanic layer is dissolved in this process so there will be little effect on the corrosion protection. But this also means that the dissolved

$Zn^{2+}_{(aq)}$ should be easily recoverable either by electrolytic recovery or precipitation. At the same time, the surface morphology will change through NaOH etching, but NaOH is already widely used in automotive manufacturing, eg, to remove surface-adsorbing additives in current metal forming lubricants (albeit the NaOH is typically at a lower concentration). Additionally, confocal microscopy shows that the macroscopic surface roughness of the NaOH-treated surfaces is similar to the as-received HDG. Because macroscopic surface roughness has a greater impact on paint appearance than roughness of smaller length scales, we do not anticipate any problems with paint adhesion or surface finish for SAM-processed substrates.

In a further interesting observation, whilst the $NaOH_{(aq)}$ treatment desorbs alkyl carboxylates and phosphonates, these are replaced by adsorbed carbonate which itself imbues similar lubricity to the substrates. This is important because while sodium carbonate is a similar price (£99 for 5 kg) to $R_{12}C$ (£70 for 5 kg), it is much cheaper than $R_{12}P$ (£54 for 1 g)—price data from Aldrich. This would also be a good end use for fossil fuel-related CO_2 removed from the atmosphere into water and, in the context of the potential impact of green lubricants, the processing methodologies described in this paper should be compatible with existing processes on assembly lines without requiring any additional steps. In addition, much less SAM material needs to be deposited compared with oil-based lubrication processes and, as stated earlier, the SAM can be recovered and re-used.

However, the mode of action of SAMs is very different to traditional lubricants because it arises from a thin, solid film on the surface rather than a liquid. Whilst a solid lubricant brings benefits in terms of reduced liquid waste, it cannot remove debris or friction-related heat from the contact area in the same way as a liquid can. However, this can be overcome by using water with the SAMs during forming rather than running them dry. As the WCA data show, the SAM surfaces are hydrophobic, and further LFT data show they work just as effectively when combined with water as when they are used dry (eg, the μ of the $R_{12}C$ samples run dry were 0.11 ± 0.005, whereas with water the μ of $R_{12}C$ was 0.12 ± 0.01). By comparison, the lubricity for the carbonated surfaces is believed to arise from carbonate acting either as an electrostatic (due to high polarity) and/or as a physical barrier coating.[30,31] The rod-like features on the NaOH (aq)-treated surface (Figure 4B) suggest that these could contribute to lowering the coefficient of friction. This is further confirmed by AFM data (ESI Figure 15) which shows no particles on the as-received DX56 surface, then many particles of 300 to 400 nm size on the $NaOH_{(aq)}$-treated surface and then that these particles are removed by sonication in water.

4 | CONCLUSIONS

This paper has shown that, not only can chemisorbed alkyl carboxylates or phosphonates act as an inherent, solid lubricants on galvanized steel, but these compounds can be easily desorbed by briefly dipping the substrates in aqueous NaOH using processes which are compatible with current steel manufacturing processes. Whilst detailed characterization confirms the desorption of the vast majority of the alkyl carboxylates or phosphonates, the coefficient of friction of the substrates does not increase as expected. Instead, not only is a significant adsorption of carbonate observed, but this new layer also appears to imbue surface lubricity. The fact that such a simple and low cost adsorbent as carbonate can influence surface properties is both important and surprising. Also, our data show that $NaOH_{(aq)}$ only etches 10% of the galvanic zinc layer which does not affect surface roughness sufficiently to affect painting or surface finish.

ACKNOWLEDGEMENTS

We gratefully acknowledge funding from EPSRC EngD and Tata Steel (D.H.), the Welsh Government for Sêr Cymru (P.J.H.), and SPACE-modules (EP/M015254/1) for E.W.J. We also acknowledge the Swansea University College of Engineering AIM Facility, which was funded by EPSRC (EP/M028267/1), the European Regional Development Fund (80708), and the Ser Solar project, both via Welssh Govt.

ORCID

Peter J. Holliman https://orcid.org/0000-0002-9911-8513

REFERENCES

1. Cheng H, Hu Y. Influence of chain ordering on frictional properties of self-assembled monolayers (SAMs) in nano-lubrication. *Adv Coll Interface Sci*. 2012;171:53.
2. Zhang Q, Wan Y, Li Y, Yang S, Yao W. Friction reducing behavior of stearic acid film on a textured aluminum substrate. *Appl Surf Sci*. 2013;280:545-549.
3. Moine MM, Roizard X, Melot J-M, et al. Grafting and characterization of dodecylphosphonic acid on copper: macro-tribological behavior and surface properties. *Surf Coat Tech*. 2013;232:567-574.
4. Newton L, Slater T, Clark N, Vijayaraghavan A. Self-assembled monolayers (SAMs) on metallic surfaces (gold and graphene) for electronic applications. *J Mater Chem C*. 2013;1(3):376-393.
5. Andrews B, Almahdali S, James K, Ly S, Crowder KN. Copper oxide surfaces modified by alkylphosphonic acids with terminal pyridyl-based ligands as a platform for supported catalysis. *Polyhedron*. 2016;114:360-369.
6. Herzer N, Hoeppener S, Schubert US. Fabrication of patterned silane based self-assembled monolayers by photolithography and surface reactions on silicon-oxide substrates. *Chem Commun*. 2010;46:5634.
7. Ulman A. Formation and structure of self-assembled monolayers. *Chem Rev*. 1996;96(4):1533-1554.
8. Raiber K, Terfort A, Benndorf C, Krings N, Henning Strehblow H. Removal of self-assembled monolayers of alkanethiolates on gold by plasma cleaning. *Surf Sci*. 2005;595(1-3):56-63.
9. Stewart A, Zheng S, McCourt MR, Bell SEJ. Controlling assembly of mixed thiol monolayers on silver nanoparticles to tune their surface properties. *ACS Nano*. 2012;6(5):3718-3726.
10. Negri P, Marotta NE, Bottomley LA, Dluhy RA. Removal of surface contamination and self-assembled monolayers (SAMs) from silver (Ag) nanorod substrates by plasma cleaning with argon. *Appl Spec*. 2011;65(1):66-74.

11. Raman A, Dubey M, Gouzman I, Gawalt ES. Formation of self-assembled monolayers of alkylphosphonic acid on the native oxide surface of SS316L. *Langmuir*. 2006;22(15):6469-6472.
12. Liu H, Bhushan B. Investigation of nanotribological properties of self-assembled monolayers with alkyl and biphenyl spacer chains. *Ultramicroscopy*. 2002;91(1-4):185-202.
13. Bhushan B, Kasai T, Kulik G, Barbieri L, Hoffmann P. AFM study of perfluoroalkylsilane and alkylsilane self-assembled monolayers for anti-stiction in MEMS/NEMS. *Ultramicroscopy*. 2005;105(1-4):176-188.
14. Van Der Linde G. Predicting galling behavior in deep drawing processes, PhD thesis, University of Twente, 2011, Ch. 1.
15. De Rooij M. Tribological aspects of unlubricated deep drawing processes, PhD thesis, 1998, University of Twente, Ch. 1.
16. Altan T, Tekkaya AE (Eds). *Sheet Metal Forming Fundamentals*. Ohio: ASM International; 2012 Ch. 7:92.
17. McIntire TM, Lea AS, Gaspar DJ, et al. Unusual aggregates from the oxidation of alkene self-assembled monolayers: a previously unrecognized mechanism for SAM ozonolysis? *Phys Chem Chem Phys*. 2005;7(20):3605-3609.
18. Hallen MA, Hallen HD. Synthesis of carboxylic acid monolayers by ozonolysis of 10-undecenyltrichlorosilane SAMs. *J Phys Chem C*. 2008;112(6):2086-2090.
19. Sun K, Jiang B, Jiang X. Electrochemical desorption of self-assembled monolayers and its applications in surface chemistry and cell biology. *J Electroanal Chem*. 2011;656(1-2):223-230.
20. Wong EHJ, May LGL, Wilde CP. Oxidative desorption of thiols as a route to controlled formation of binary self-assembled monolayer surfaces. *Electrochim Acta*. 2013;109:67-74.
21. Choi S, Chae J. A regenerative biosensing surface in microfluidics using electrochemical desorption of short-chain self-assembled monolayer. *Microfluid Nanofluids*. 2009;7(6):819-827.
22. Holliman PJ, Al-Salihi KJ, Connell A, Davies ML, Jones EW, Worsley DA. Development of selective, ultra-fast multiple co-sensitization to control dye loading in dye-sensitized solar cells. *RSC Adv*. 2014;4(5):2515-2522.
23. Hill D, Holliman PJ, McGettrick J, et al. Study of the tribological properties and ageing of alkyphosphonic acid films on galvanized steel. *Tribol Internat*. 2018;119:337-344.
24. Hill D, Holliman PJ, McGettrick J, et al. Studies of inherent lubricity coatings for low surface roughness galvanised steel for automotive applications. *Lubricat Sci*. 2017;29(5):317-333.
25. http://lisa.chem.ut.ee/IR_spectra
26. Sahoo RR, Biswas SK. Frictional response of fatty acids on steel. *J Coll Interface Sci*. 2009;333(2):707-718.
27. Kutscher JS, Gericke A, Huhnerfuss H. Effect of bivalent Ba, Cu, Ni, and Zn cations on the structure of octadecanoic acid monolayers at the air-water interface as determined by external infrared reflection-absorption spectroscopy. *Langmuir*. 1996;12(4):1027-1034.
28. van den Brand J, Blajiev O, Beentjes PCJ, Terryn H, de Wit JHW. Interaction of anhydride and carboxylic acid compounds with aluminum oxide surfaces studied using infrared reflection absorption spectroscopy. *Langmuir*. 2004;20(15):6308-6317.
29. Paz A, Guadarrama D, López M, E. González J, Brizuela N, Aragón J. A comparative study of hydroxyapatite nanoparticles synthesized by different routes. *Quím Nova*. 2012;35(9):1724-1727.
30. Jin D, Yue L. Tribological properties study of spherical calcium carbonate composite as lubricant additive. *Mater Lett*. 2008;62(10–11):1565-1568.
31. Ji X, Chen Y, Zhao G, Wang X, Liu W. Tribological properties of $CaCO_3$ nanoparticles as an additive in lithium grease. *Tribol Lett*. 2011;41(1):113-119.
32. Thissen P, Vega A, Peixoto T, Chabal YJ. Controlled, low-coverage metal oxide activation of silicon for organic functionalization: unraveling the phosphonate bond. *Langmuir*. 2012;28(50):17494-17505.
33. Plasencia A, Piasecki JD, Strohmeier BR. XPS surface characterization of disposable laboratory gloves and the transfer of glove components to other surfaces. *Spectroscopy*. 2012;27:36.
34. Bhure R, Mahapatro A, Bonner C, Abdel-Fattah TM. In vitro stability study of organophosphonic self assembled monolayers (SAMs) on cobalt chromium (Co–Cr) alloy. *Mater Sci Eng C*. 2013;33(4):2050-2058.
35. Wijenberg J, Oroog J. Dezincing of zinc alloy coated steel scrap in hot caustic soda. *Steel Res*. 1999;70(6):227-232.
36. Li H, Belkind A, Jansen F, Orban Z. An in situ XPS study of oxygen plasma cleaning of aluminum surfaces. *Surf Coat Tech*. 1997;92(3):171-177.

SUPPORTING INFORMATION

Additional supporting information may be found online in the Supporting Information section at the end of the article.

How to cite this article: Hill D, Holliman PJ, Jones EW, et al. Desorption of carboxylates and phosphonates from galvanized steel: Towards greener lubricants. *Surf Interface Anal*. 2019;1–9. https://doi.org/10.1002/sia.6681